Xu et al. Biochar (2026) 8:108
https://doi.org/10.1007/s42773-026-00627-7

Biochar

REVIEW Open Access

Colloidal stability of dissolved black carbon: interfacial mechanisms and environmental implications

Fanchao Xu[1,2], Jun Zhu[1], Kun Liu[3*], Minli Wang[4], Huiting Liu[5], Jianjun Lian[1], Xiaolei Qu[2] and Bingyu Wang[6*]

Abstract

Dissolved black carbon (DBC) plays a critical role in carbon sequestration, pollutant transport, and environmental remediation, as the colloidal stability of DBC governs both its own environmental fate and that of adsorbed pollutants. However, the mechanistic understanding of DBC colloidal stability remains a key knowledge gap, meaning that its controlling factors and environmental implications are also poorly understood. This review comprehensively examines the evolution of molecular structures and chemical compositions that determine DBC colloidal stability. By comparing the relative contributions and trends of the dominant interfacial forces using DLVO/XDLVO theory, it elucidates the control mechanisms governing its colloidal stability and identifies key factors responsible for behavioral variations. The colloidal behavior of DBC influences its speciation and bioavailability, altering its ecological risk in aquatic systems. Additionally, the colloidal stability of DBC governs its interactions with pollutants, thereby directly governing their transport and fate. Furthermore, aggregation-deposition processes sequester DBC and associated pollutants in sediments, reducing estuarine vertical flux and ultimately impacting the global carbon cycle. Future research should focus on developing integrated characterization techniques to provide reliable and comparable multidimensional structural information for DBC, investigating structure-dependent heteroaggregation mechanisms in complex environmental matrices, and developing robust predictive models for its colloidal behavior.

Highlights

- Key structural determinants of DBC colloidal stability were reviewed.
- Interfacial mechanisms of DBC colloidal stability were critically discussed.
- Primary factors responsible for DBC colloidal behavior were generally summarized.
- Environmental implications of DBC colloidal stability were highlighted.
- Future prospects regarding DBC colloidal stability were outlined.

Keywords Dissolved black carbon, Colloidal behavior, XDLVO theory, Pollutant transport, Ecological risk

*Correspondence:
Kun Liu
kunliu@smail.nju.edu.cn
Bingyu Wang
bingyuwang@njust.edu.cn
Full list of author information is available at the end of the article

Springer

Graphical Abstract

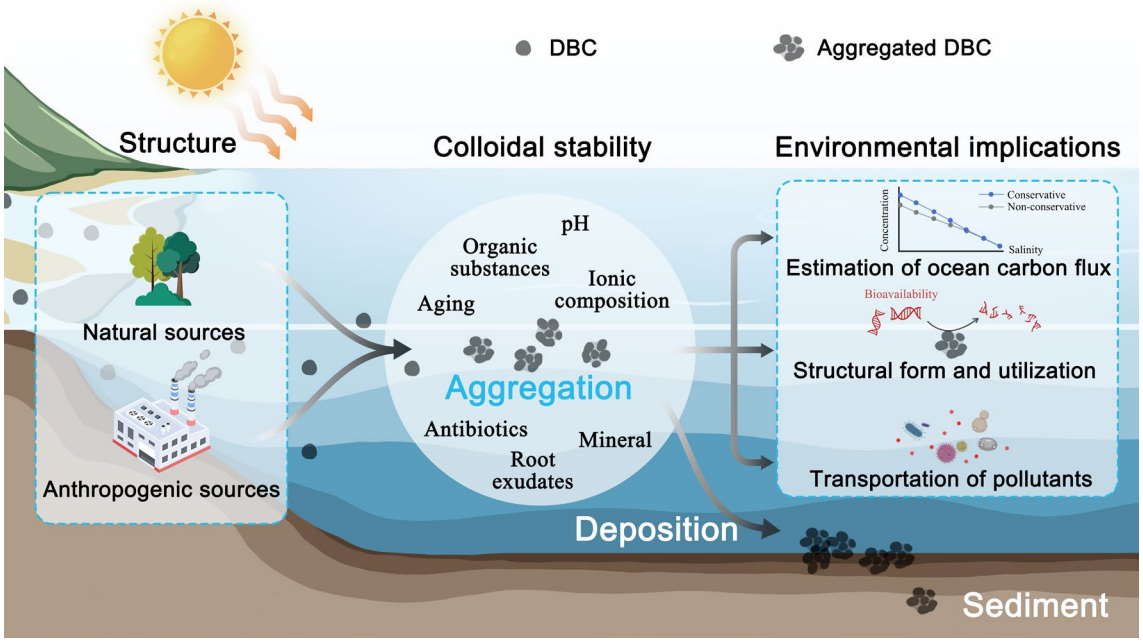

1 Introduction

Black carbon (BC) is produced during the incomplete combustion of fossil fuels and biomass (Eckhardt et al. 2023; Li et al. 2024d; Wang et al. 2025). The increasing frequency of wildfires worldwide and the substantial input of biochar have contributed to a growing flux of BC into terrestrial ecosystems (Wang et al. 2023b; Xu et al. 2024). Dissolved BC (DBC), operationally defined as the water-soluble fraction of BC that passes through a filter (0.1 – 0.70 μm) (Coppola et al. 2022), exhibits high environmental mobility. It can be readily released from BC residues by leaching and surface runoff and extensively transported from soils to aquatic systems. However, the molecular definition of DBC varies substantially across studies, depending on whether the analytical approach targets the condensed aromatic structures or the entire suite of DOC molecules leached from BC. This divergence reflects the broad diversity of structural components assigned to DBC, ranging from condensed aromatic structures rich in polar groups to larger molecular structures containing aliphatic-like, carbohydrate-like, and other non-condensed components (Fan et al. 2025; Fang et al. 2022; Qu et al. 2016). Consequently, DBC exhibits highly condensed polycyclic aromatic structures that account for its higher aromatic carbon relative to aquatic dissolved organic matter (DOM), while its surface is more enriched with polar carboxyl groups than terrestrial DOM (Qu et al. 2016). These structures enable DBC to constitute a distinct and critical portion of DOM (Tang et al. 2024; Zhou et al. 2025). DBC is widely distributed across natural aquatic systems, including oceans, bays, lakes, rivers, and estuaries (Bao et al. 2017; Lu et al. 2024; Yin et al. 2023). Given its strong sorption affinity and colloidal stability, DBC can act as an efficient long-range carrier for assorted pollutants in aquatic systems, thereby influencing the global carbon cycle and climate change, and posing potential risks to human health (Hu et al. 2025; Seelen et al. 2023; Yamashita et al. 2022).

The molecular structure of DBC is generally characterized by its high aromaticity and abundant oxygen-containing functional groups (Roebuck et al. 2018; Wang et al. 2020). Among these, the aromatic and oxygenated functional groups of DBC are important binding sites for organic pollutants and heavy metals (Roebuck et al. 2018; Wang et al. 2023a). Therefore, it is an active medium in the environment that influences the distribution of and response to pollutants. Anthropogenically produced BC (biochar) has received increasing attention as a soil amendment because of its advantages in terms of carbon sequestration, soil productivity, and pollutant immobilization (Hameed et al. 2023; He et al. 2024; Lian and Xing 2024; Xiang et al. 2022). However, DBC released from

biochar may act as a mobile carrier for adsorbed pollutants, potentially compromising the effectiveness of biochar in soil remediation applications (Hao et al. 2025; Lian and Xing 2024). Therefore, understanding the fate and reactivity of DBC is crucial for not only predicting contaminant behavior but also evaluating the potential risks associated with biochar-based soil remediation.

Processes such as aggregation and deposition are colloidal behaviors that often occur at the interface of DBC during environmental transport (Song et al. 2019; Tang et al. 2024; Yang et al. 2019). The colloidal stability of DBC has profound implications for its own environmental fate and that of priority pollutants. The colloidal behavior of DBC influences its speciation and bioavailability in aquatic systems, reduces carbon flux through sediment sequestration, and ultimately impacts climate change (Garnett et al. 2021; Lian et al. 2020; Wang et al. 2024). Notably, the aggregation behavior of DBC in fluvial and estuarine systems may induce its fractionation from the dissolved organic carbon pool through aggregation processes, potentially leading to its accumulation in terrestrial sediments as a significant intermediate reservoir (Xu et al. 2017; Yamashita et al. 2022). Carbon isotopic analyses have further revealed the inherent instability of riverine DBC during its marine transit, exhibiting marked flux attenuation in estuarine zones (Qi et al. 2020; Yin et al. 2023). Structurally, DBC exhibits source-specific molecular heterogeneity that undergoes progressive transformation during biogeochemical cycling. This structural divergence shows strong covariation with the pyrolysis temperature and lignin composition; increasing pyrolysis temperatures degrade oxygen-containing functionalities but increase aromatic condensation and molecular weight, whereas elevated lignin proportions facilitate environmental mobility through enhanced colloidal stability (Han et al. 2021; Yan et al. 2023; Yang et al. 2019). Photoaging processes further modify the characteristics of DBC by increasing the oxygen-containing moieties, thereby enhancing its colloidal stability and altering its environmental transport pathways (Fu et al. 2016; Li et al. 2024a; Wang et al. 2023a). Despite these advances, recent studies have disproportionately emphasized the discrete facets of the colloidal behavior of DBC, including its molecular architecture, ionic interactions, and photochemical effects. However, there remains a significant gap in a comprehensive review of the mechanistic understanding of DBC colloidal stability and its environmental implications, knowledge that is essential for understanding the environmental fate of DBC and assessing priority pollutant risks.

Previous review articles have explored the structural characteristics of DBC and its role in environmental remediation, pollutant interactions, migration, and transformation mechanisms (Fan et al. 2025; Hameed et al. 2023; Lian and Xing 2024; Yao et al. 2025), while the critical role of colloidal stability during environmental transport and interfacial processes has been neglected. Thus, significant knowledge gaps remain regarding the colloidal stability of DBC and its molecular chemical structure, governing mechanisms, and related environmental implications. Addressing these gaps is essential for improving the estimation of carbon fluxes and the assessment of priority pollutant risks. This review aims to provide an in-depth understanding of the structure and molecular composition of DBC as well as its colloidal behavior mechanisms, controlling factors, and to systematically discuss its environmental implications. The primary objectives of this review are (1) to elucidate the influence of the source materials and formation pathways of DBC on its structural and molecular composition characteristics that directly govern its colloidal stability; (2) to advance the mechanistic understanding of DBC colloidal stability through the DLVO/XDLVO framework by clarifying the dominant interfacial forces; and (3) to identify controlling factors and environmental implications of DBC colloidal stability, thereby outlining corresponding research directions for future studies. Through these efforts, this review establishes a reference framework for understanding the structural characterization and colloidal stability of DBC, with the objective of providing new perspectives on its environmental fate and the assessment of pollutant risks.

2 Source materials, formation pathways, and structural characteristics of DBC

Analysis of the molecular structures and chemical compositions of DBC is crucial for understanding its colloidal and biogeochemical behaviors. DBC, defined as the water-soluble fraction of the black carbon continuum, consists of a wide range of organic compounds with varying stoichiometric ratios and structural configurations (Qu et al. 2016; Yin et al. 2023). Its chemical and molecular compositions are dependent upon the feedstock source, pyrolysis conditions, and extraction conditions, which are summarized in Table S1. Various analytical techniques have been employed to characterize the molecular structure of DBC. Molecular and surface composition analyses have primarily been conducted using elemental analysis (EA), ultraviolet–visible spectroscopy (UV–Vis), excitation-emission matrix spectroscopy (EEM), and X-ray photoelectron spectroscopy (XPS) (Chen et al. 2022a; Zhang et al. 2024a). Transmission electron microscopy, Fourier-transform infrared (FT-IR) spectroscopy, and nuclear magnetic resonance (NMR) spectroscopy have been employed to elucidate

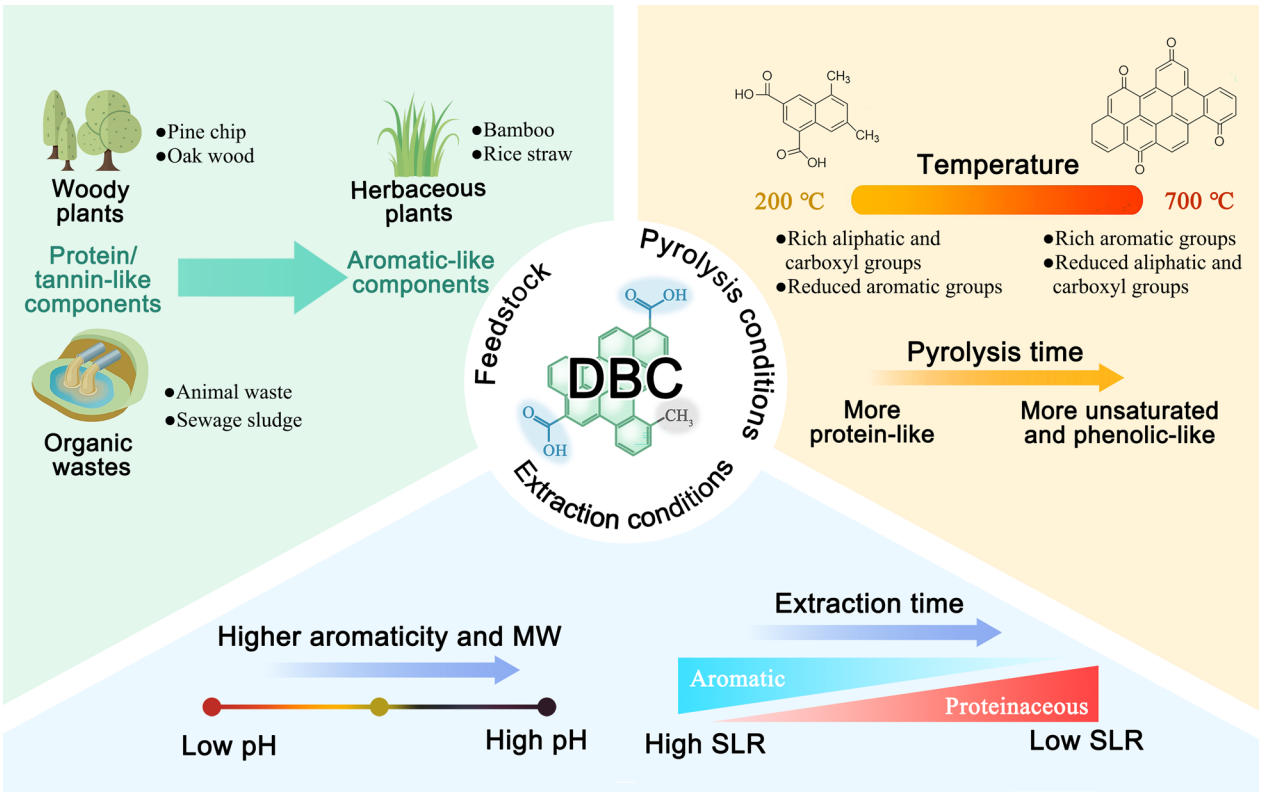

Fig. 1 Effect of feedstock source, pyrolysis, and extraction conditions on the chemical structure of DBC. Where the SLR represents biochar/extraction solution ratio

the structure and morphology of DBC (Li et al. 2024b; Wang et al. 2024). In addition, the partition coefficient of DBCs in aqueous two-phase systems provides an effective method for characterizing their hydrophobicity (Fu et al. 2019; Liu et al. 2019b). Recent advances have enabled molecular-level characterization of the structural properties of DBC using electrospray ionization Fourier-transform ion cyclotron resonance mass spectrometry (FT-ICR MS) (Li et al. 2024a; Sun et al. 2025). In conclusion, the abovementioned analytical techniques are useful for characterizing the molecular structure of DBC. However, each technique has certain limitations. The integration of multiple techniques is imperative to enhance reliability, eliminate analytical uncertainties, and advance the mechanistic understanding of the molecular structure of DBC and its environmental functions (Hameed et al. 2023).

2.1 Feedstock source

The feedstock source for DBC significantly affects its leaching and chemical structure (Fig. 1). More DBC is released from herbaceous (cellulose/hemicellulose-rich) plant biochar than from woody (lignin-rich) plant biochar (Mukherjee and Zimmerman 2013). The recalcitrance of lignin is attributed to its aromatic-rich structure, which impedes its biotic and abiotic degradation (Kim et al. 2020). Among herbaceous plants, bamboo produces DBC with a higher carbon content (13.00 wt.%) than that of DBC produced by rice (7.71 wt.%), suggesting that a higher ash content in virgin biochar significantly affects the production of DBC in biochar (Wei et al. 2020a). Solid-state ^{13}C NMR analysis has shown that DBC produced from bamboo differs significantly from that produced from rice in terms of its chemical structure (e.g., aromatic carbon, alkyl, O-alkyl, and C=O) (Qu et al. 2016), whereas DBC extracted from rice straw biochar has more aromatic carbon components than that extracted from pine wood, swine, and sewage sludge (as shown in Fig. 2a) (Wei et al. 2019). In addition, polycyclic aromatic and protein/tannin components are more abundant in DBC produced by woody plant biochar than that produced by other types of biochar (Liu et al. 2022b; Rajapaksha et al. 2019; Yamashita et al. 2022). These studies have shown that different feedstocks lead to differences in the structural properties of DBC, especially the aromatic and protein/tannin-like components.

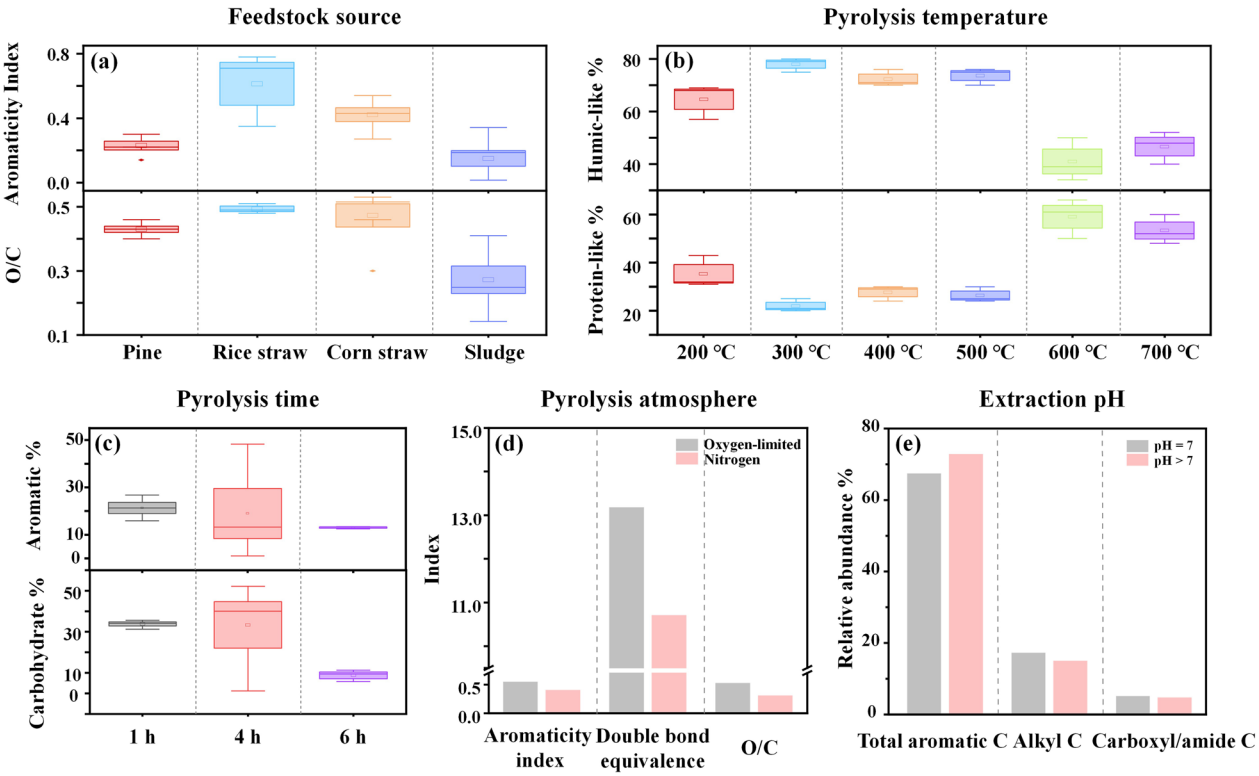

Fig. 2 The chemical and molecular compositions of DBC under different **a** feedstock sources, **b** pyrolysis temperatures, **c** pyrolysis time, **d** pyrolysis atmospheres and **e** extraction pH. The data of **a–e** were adapted from references (Gui et al. 2020; Hu et al. 2023; Ji et al. 2024; Li et al. 2024a; Liu et al. 2019a; Song et al. 2020; Sun et al. 2025; Wang et al. 2023a; Wei et al. 2020a; Zhang et al. 2024a, 2020, 2024b)

2.2 Pyrolysis conditions

The leachability and structural properties of DBC are predominantly regulated by the pyrolysis conditions, including the pyrolysis temperature, heating rate, and duration. The chemical and molecular compositions of DBC under different pyrolysis temperatures, durations, and atmospheres are illustrated in Fig. 2b–d, respectively. The pyrolysis temperature is generally recognized as a more critical factor than the pyrolysis rate, and the functional groups, aromaticity, and humification degree of DBC are strongly correlated with the pyrolysis temperature during DBC formation (Fig. 1) (Chen et al. 2022a; Du et al. 2022; Huang et al. 2021; Lian and Xing 2017). The concentration of DBC produced at higher pyrolysis temperatures is significantly lower than that produced at lower temperatures due to enhanced aromatization and polymerization (Song et al. 2023; Taherymoosavi et al. 2018; Zhang et al. 2020). In addition, a high pyrolysis temperature leads to a decrease in the content of C=O groups and an increase in the content of quinone groups in DBC (Chen et al. 2022a), e.g., the content of graphitized carbon of DBC pyrolyzed at 500 °C is twice as high as that of raw biomass (Chen et al. 2022b). Advanced FT-ICR MS has recently provided molecular-level insights into the effects of the pyrolysis temperature on the DBC structure. The results show a decrease in the H/C ratio of DBC from 200 °C to 500 °C, at which a significant increase is observed in the condensed aromatic carbonyl compounds with narrow molecular weight distributions, which show smaller molecular ranges and higher aromaticity (Chang et al. 2020; Li et al. 2024a). Moreover, biochar produced at higher pyrolysis rates yields DBC with elevated organic carbon content, attributable to incomplete biomass pyrolysis from shorter residence times. This incomplete pyrolysis retains a potentially bioavailable carbon source, thereby increasing the organic carbon yield (Jamieson et al. 2014; Sun et al. 2021; Yang et al. 2018).

2.3 Extraction conditions

The structural characteristics of DBC are also significantly related to the extraction conditions, such as the pH of the extraction environment, solid/liquid ratio (biochar/extraction solution ratio, SLR), and extraction time (Li et al. 2017; Liu et al. 2019a; Wu et al. 2018). Studies have confirmed that under the same conditions, the content of DBC extracted from an acidic solution is lower (16.3 g kg^{-1}) than that from an alkaline solution (22.8 g kg^{-1}). Similar reports have demonstrated that straw biochar can produce up to 5000 mg kg^{-1} of DBC under 0.1 M NaOH (Li et al. 2017). This difference may

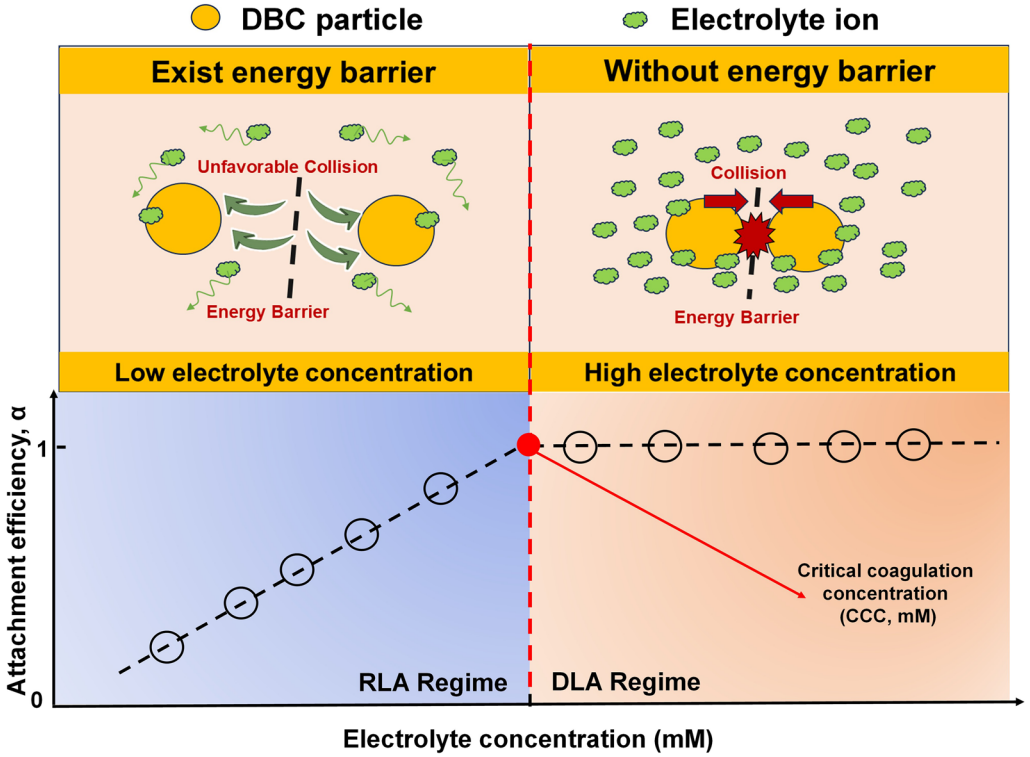

Fig. 3 Schematic illustration of the critical coagulation concentration (CCC), which was determined by the electrolyte concentration at the intersection of the reaction-limited stability curve ($\alpha < 1$) (Reaction-Limited Aggregation (RLA) regime with an energy barrier) and the diffusion-limited stability curve ($\alpha = 1$) (Diffusion-Limited Aggregation (DLA) regime, without energy barrier)

be due to the enhanced hydrophilicity imparted by the deprotonation of acidic functional groups at elevated pH (Wu et al. 2018). Further, alkali extraction may promote the hydrolysis reaction on the surface of biochar in solution, resulting in greater solubilization of the hydrocarbon organic carbon, which has higher aromaticity and molecular weight (Fig. 2e). The released DBC may come from acidic functional groups, which are closely related to the degree of surface oxidation (Liu et al. 2019a; Song et al. 2020; Sun et al. 2021). In addition, the content and structural properties of DBC are affected by the extraction solid–liquid ratio and extraction time. When the SLR is decreased from 1:2 to 1:10 and the extraction time is increased from 10 to 300 min, the contents of extracted DBC proteinaceous components increase significantly, while those of fulvic- and humic-like compounds increase more moderately (Xie et al. 2017).

3 Colloidal stability and governing mechanisms of DBC

3.1 Colloidal stability and analytical methods

As a key interfacial attribute, colloidal stability controls DBC fate in aquatic systems. The aggregation and subsequent deposition regulate both the transport flux of DBC and the environmental fate of the adsorbed contaminants. Time-resolved dynamic light scattering (*t*-DLS) measurements are commonly employed to study the aggregation behavior of DBC. The attachment efficiency (α) is a key metric for quantifying the tendency of DBC particle aggregation in a given water chemistry (Tang et al. 2024; Xing et al. 2023; Xu et al. 2017). It is determined by normalizing the initial aggregation rate in the solution of interest to that in the Diffusion-Limited Aggregation (DLA) regime, where the aggregation rate constant is independent of the electrolyte concentration (Equation [1]) (Xu et al. 2017).

$$\alpha = \frac{\left(\frac{dd_h(t)}{dt}\right)_{t\to 0}}{\left(\frac{dd_h(t)}{dt}\right)_{t\to 0,fast}} \quad (1)$$

where $d_h(t)$ is the intensity-weighted average hydrodynamic diameter measured by the *t*-DLS. The value of $\left(\frac{dd_h(t)}{dt}\right)_{t\to 0}$ is determined by applying linear least-squares regression analysis to the initial phase of the aggregation curve (i.e., hydrodynamic radius as a function of time). Subscript "fast" represents the DLA conditions. $\left(\frac{dd_h(t)}{dt}\right)_{t\to 0,fast}$ is the average of the initial slopes of

all aggregation kinetic curves gained under the DLA regime. A higher α value suggests a less stable colloidal system (Xin et al. 2023; Xu et al. 2017). Stability curves can be established by plotting α as a function of the electrolyte concentration. The critical coagulation concentration (CCC) can be determined at the electrolyte concentration where the DLA regime was achieved, as illustrated in Fig. 3. The CCC value serves as a quantitative metric to compare DBC colloidal stability in various solution chemistry. In the DLA regime at concentrations exceeding the CCC, DBC particles overcome the repulsive energy barrier, with each collision resulting in adhesion and leading to rapid aggregation (Fig. 3) (Yang et al. 2019). The CCC values of DBC reveal its distinct aggregation behavior in relation to conventional DOM fractions (Fang et al. 2020; Liu et al. 2018). For divalent cations such as Ca^{2+}, the CCC of DBC typically ranges between 38.1 mM and 75 mM (Xu et al. 2017; Yang et al. 2019). This range is notably lower than that of aquatic DOM (e.g., 46.9–110.4 mM for various reference humic and fulvic acids) but substantially higher than that of terrestrial DOM fractions (e.g., 1.96–4.88 mM for soil and peat humic acids) (Wei et al. 2020b). This phenomenon may be attributed to the chemical composition of DBC. It exhibits higher aromatic carbon and lower aliphatic carbon than aquatic DOM, promoting hydrophobicity and aggregation. Concurrently, DBC is richer in polar carboxyl groups than terrestrial DOM, which enhances hydrophilicity and colloidal stability (Fu et al. 2016; Lian and Xing 2024; Xu et al. 2017). In addition to *t*-DLS measurements, quartz crystal microbalance with dissipation monitoring (QCM-D) was employed to characterize the colloidal stability of DBC and has been widely applied to investigate DBC deposition on various sensor surfaces (Ou et al. 2021; Xu et al. 2020). For example, the QCM-D results indicated that heavy metal cations (e.g., Pb^{2+}) significantly enhance DBC aggregation and deposition on silica substrates (Xu et al. 2020). The same phenomenon has been observed for Ca^{2+} systems, where enhanced DBC aggregation with increasing ionic strength causes sequential layer stiffening followed by softening (Ou et al. 2021).

3.2 Governing mechanisms and theoretical model

The colloidal behavior of DBC and its underlying mechanisms are typically interpreted using both the classical colloidal stability (Derjaguin-Landau-Verwey-Overbeek, DLVO) theory and its extended form (XDLVO theory). DLVO theory posits that particle aggregation thermodynamics are governed by London-van der Waals (LW) and electrostatic interactions (Mohona et al. 2019; Van Oss 2003). As electrostatic forces generally

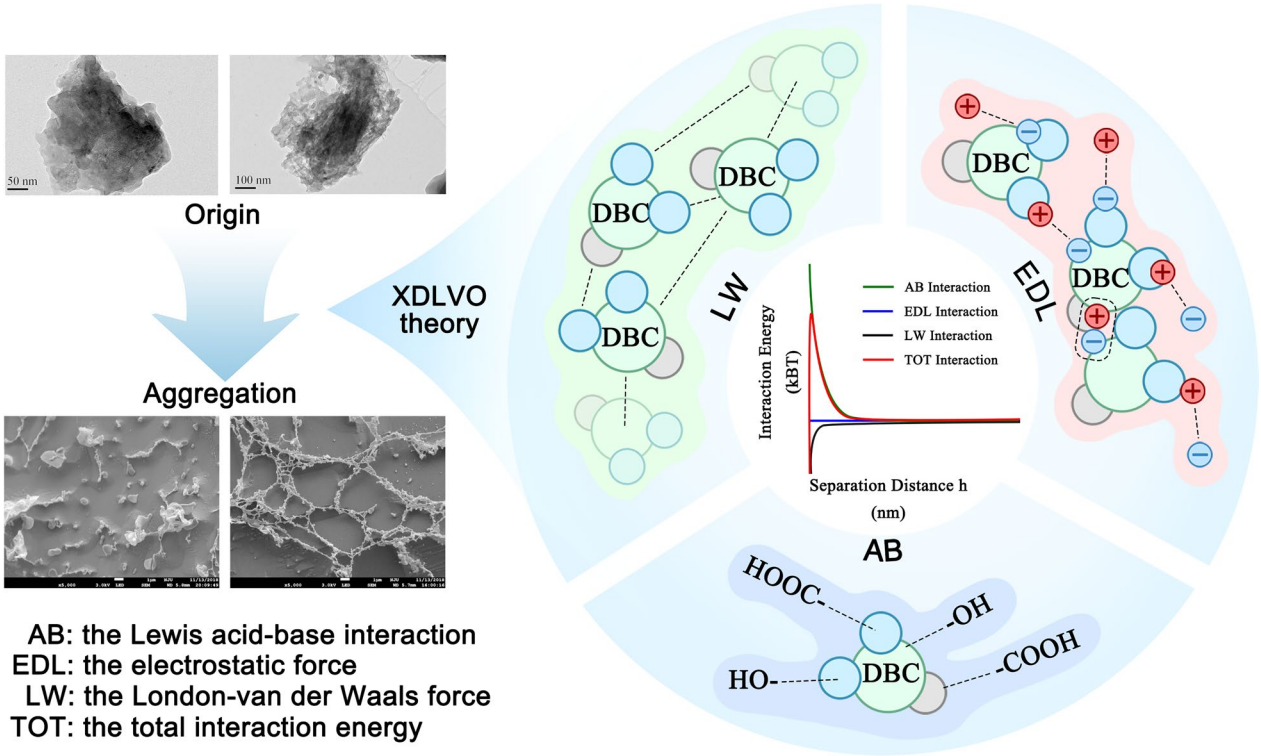

Fig. 4 Mechanistic insights into the colloidal dynamics of DBC. Some insets were adapted from references (Xu et al. 2017) and (Xu et al. 2019)

manifest as repulsive barriers against aggregation, the surface charge predominantly determines the particle aggregation behavior (Chen and Elimelech 2009). For instance, DLVO-based calculations of interaction energies for wheat straw-derived DBC in NaCl solutions have shown that increasing the NaCl concentration from 40 to 150 mM compresses the electrical double layer, thus reducing the electrostatic repulsion and promoting aggregation, which is consistent with experimental aggregation kinetics (Yang et al. 2022). Similarly, under varying pH conditions (5, 7, and 9), DBC demonstrates progressive reduction of both surface charge and colloidal stability at elevated NaCl concentrations. The observed aggregation behavior follows the classical DLVO theory, exhibiting distinct RLA and DLA regimes (Tang et al. 2024). However, the classical DLVO theory fails to describe DBC aggregation adequately in specific scenarios, particularly with divalent cations (e.g., Mg^{2+} and Ca^{2+}) (Ou et al. 2021; Yang et al. 2019). Notably, despite significant surface charge reduction (evidenced by near-neutral zeta potentials) in high-concentration NaCl and $MgCl_2$ solutions due to charge screening, bamboo-derived DBC maintains colloidal stability without aggregation, indicating that electrostatic repulsion alone cannot explain its persistent stability (Xu et al. 2017). The XDLVO theory is typically employed to calculate the total interaction energy (TOT) for compare the relative contributions and trends of the dominant interfacial forces of DBC particles under varying aqueous chemical conditions as demonstrated in Fig. 4. The consistent correlation observed between the calculated interaction energy profiles and the macroscopic aggregation behavior of DBC suggests that the XDLVO approach offers a valid thermodynamic perspective to elucidate the governing forces, while it is recognized that surface heterogeneity and possible short-range specific interactions are factors that could be addressed by combining microscopic simulations in future research. The TOT interaction represents the sum of the LW force, electrostatic force (EDL), Lewis acid–base (AB) interactions and Brownian movement force (BR) (Van Oss 2006). Notably, within the classical XDLVO framework, when LW, EDL and AB interactions are measured separately, and the TOT interaction is measured as a whole by interfacial tension determination, then BR is inherently included (Azeredo et al. 1999; Van Oss 2006). The TOT interaction energy can be obtained from Equation [2] (Van Oss 1995; Wang et al. 2013a).

$$\Phi^{Total} = \Phi^{LW} + \Phi^{EDL} + \Phi^{AB} \tag{2}$$

Equations [3], [4], and [5] can be employed to calculate the LW interaction energy (Φ^{LW}), electrostatic interaction energy (Φ^{EDL}), and Lewis AB interaction energy (Φ^{AB}) of DBC, respectively (Xu et al. 2017):

$$\Phi^{LW} = -\frac{A}{6}\left[\frac{2a_p{}^2}{h^2+4a_ph} + \frac{2a_p{}^2}{h^2+4a_ph+4a_p{}^2} + ln\left(\frac{h^2+4a_ph}{h^2+4a_ph+4a_p{}^2}\right)\right] \tag{3}$$

where A is the Hamaker constant, a_p is the radius of DBC particles, h is the separation distance between the surfaces.

$$\Phi^{EDL} = 2\pi\varepsilon_0\varepsilon_w a_p\psi_p{}^2 exp(-\kappa h) \tag{4}$$

where ε_0 is the dielectric permittivity of vacuum, ε_w is the dielectric constant of water, ψ_p is the ζ-potential of DBC particles, κ is the inverse of Debye length.

$$\Phi^{AB} = \pi a_p\lambda_w\Delta G_{h_0}^{AB} exp\left(\frac{h_0-h}{\lambda_w}\right) \tag{5}$$

where λ_w is the characteristic decay length of AB interactions in water (1.0 nm at 20 °C) (Wang et al. 2013a) and $\Delta G_{h_0}^{AB}$ represents the Lewis acid–base (AB) interaction free energy per unit area corresponding to h_0.

Φ^{LW} is a general attractive interaction between DBC particles that decays very steeply with distance and is primarily governed by the Hamaker constant. Φ^{EDL} typically manifests as a repulsive force that creates an energy barrier between DBC particles and is one of the key forces maintaining colloidal stability. It is strongly dependent on the surface charge of DBC particles and the ionic strength of the solution. In contrast, Φ^{AB} accounts for acid–base (polar) interactions, which can occur in both attractive (hydrophobic interaction) and repulsive (hydration pressure) modes with a rather steep exponential decay rate, and exhibits strong dependence on the surface hydrophilicity/hydrophobicity of DBC (Van Oss 2006). XDLVO interaction analysis has revealed that the high colloidal stability of DBC in Na^+ and Mg^{2+} solutions is correlated with the substantial energy barrier provided by hydration forces. Both Na^+ and Mg^{2+} exhibit limited capacities to suppress hydration forces, merely reducing the intermolecular electrostatic repulsion through charge screening effects. Those effects induce the structural compression of DBC without triggering aggregation (Dhangar et al. 2023; Xu et al. 2017). In contrast, Ca^{2+} and Ba^{2+} destabilize DBC by complexing with its oxygen-containing functional groups, thereby reducing hydrophilicity, weakening the hydration forces, and enhancing DBC aggregation (Kloster et al. 2013; Tang et al. 2024; Xu et al. 2017). In addition, the XDLVO theory further elucidates the aggregation behavior of different DBC types. The maximum repulsion energy barrier between the DBC particles produced at various pyrolysis temperatures decreases with increasing NaCl or $CaCl_2$ concentration until the CCC is reached. The CCC of cellulose-rich DBC falls

between those of lignin-rich and organic matter-rich DBC, indicating that the carbon content of the feedstock is a key factor governing the colloidal stability of DBC derived from different biochars (Li et al. 2023a). Furthermore, elevated pyrolysis temperatures reduce the CCC by increasing the surface hydrophobicity of DBC, which enhances the attractive Lewis AB interactions governing particle aggregation (Yang et al. 2019).

Collectively, the governing mechanisms of DBC colloidal stability can be effectively elucidated within the DLVO/XDLVO thermodynamic framework, as evidenced by the consistent correlation between calculated interaction energy profiles and macroscopic aggregation behaviors. The LW interaction provides a constant attractive force. The long-range EDL interaction establishes the primary repulsive energy barrier, the height of which is finely tuned by aqueous chemistry, thereby controlling the aggregation kinetics. Ultimately, the short-range AB interaction is the key force determining DBC colloidal stability in that it can reinforce stability through strong hydrophilic repulsion or switch to an attractive force that facilitates aggregation when surface hydrophilicity is compromised. Notably, AB interactions may achieve energies up to two orders of magnitude higher than the LW and EDL interactions (Van Oss 2006; Xu et al. 2017).

4 Controlling factors of DBC colloidal behavior

The colloidal behavior of DBC in aquatic systems is regulated by multiple factors, including ionic composition, pH, organic substances, minerals, and aging processes. The following subsections detail how each factor modulates the interfacial interactions governing DBC aggregation and colloidal stability. Collectively, these factors determine the interfacial forces between DBC particles, thereby controlling the environmental mobility of DBC and its role in the transport of pollutants.

4.1 Ionic composition

The characteristics of cations (valence and hydration radius) in solution determine the fate of DBC in aquatic systems through ion-specific aggregation pathways. Monovalent cations (e.g., Na^+) exhibit limited aggregation effects. Wheat-straw-derived DBC shows a decreased CCC at higher pyrolysis temperatures owing to the reduced content of oxygen-containing functional

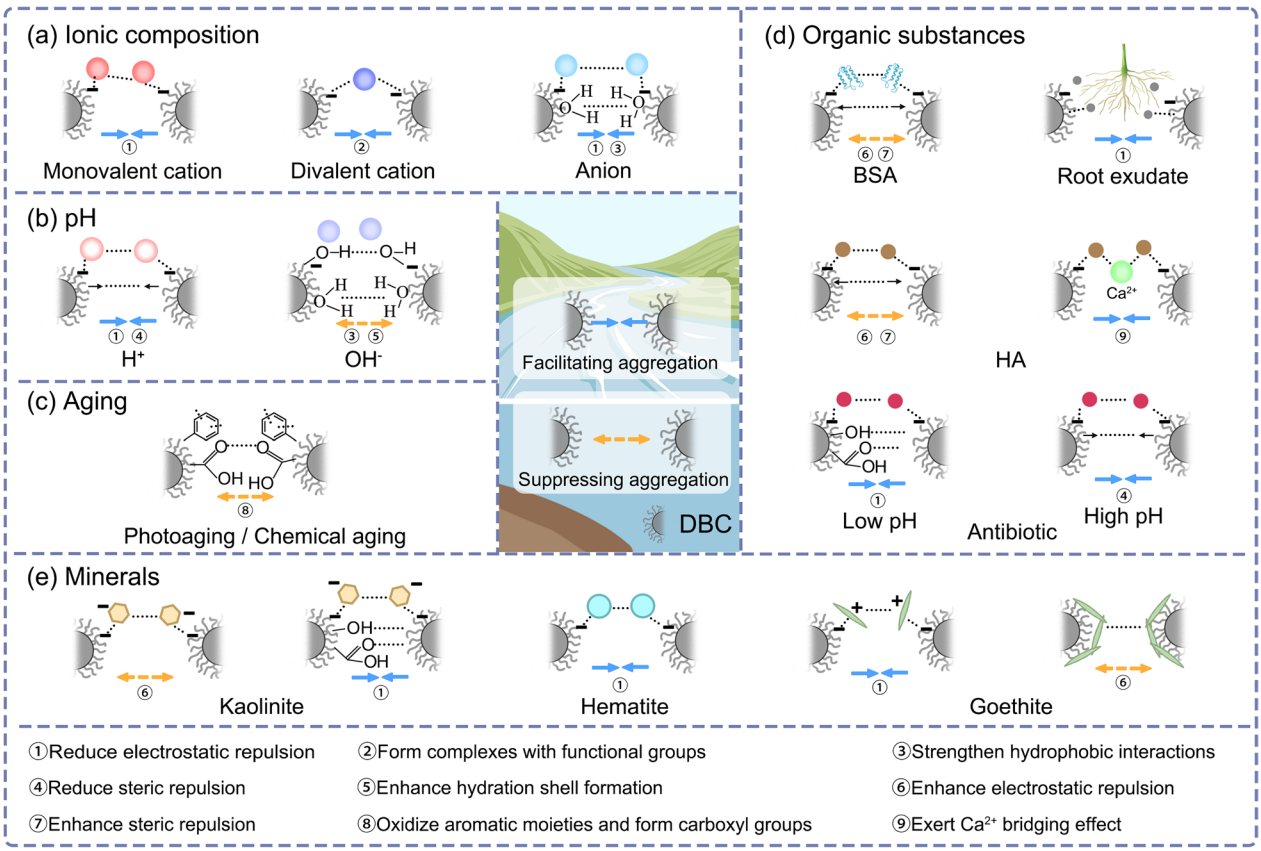

Fig. 5 The controlling factors include **a** ionic composition, **b** pH, **c** aging, **d** organic substances, and **e** minerals, along with their corresponding mechanisms and implications for the colloidal behavior of DBC in aquatic systems

groups and consequent lower surface charge density (Ou et al. 2021; Yang et al. 2019). In contrast, bamboo-derived DBC demonstrates exceptional stability, even at high Na^+ concentrations (800 mM), where hydration forces dominate colloidal stabilization, as evidenced by the XDLVO theory (Xu et al. 2017). These divergent behaviors likely originate from source-dependent variations in the chemical composition of DBC. Divalent cations induce more pronounced aggregation than monovalent cations (Dhangar et al. 2023; Xu et al. 2017; Yang et al. 2019). Environmentally relevant divalent cations exhibit distinct aggregation potentials for DBC, with destabilization capacity in the order of $Ba^{2+} > Ca^{2+} \gg Mg^{2+}$ (Dhangar et al. 2023; Xu et al. 2017). Ca^{2+}/Ba^{2+} enhance DBC hydrophobicity through strong complexation with oxygen-containing functional groups. Additionally, these cations further promote aggregation via bridging effects (Fang et al. 2025; Kloster et al. 2013; Xia et al. 2024). In contrast, Mg^{2+} exhibits weaker aggregation capacity due to limited carboxyl complexation, resulting in high energy barriers and thereby limited influence on DBC aggregation (Xu et al. 2017). Divalent heavy metal cations also significantly affect aggregation by undergoing strong metal–oxygen functional group complexation and cation-π interactions with DBC (Dhangar et al. 2023; Huang et al. 2021; Xu et al. 2020). Their destabilization capacity (CCC in the order $Zn^{2+} > Cd^{2+} > Cu^{2+} > Pb^{2+}$) correlates with their electronegativity (Huang et al. 2021; Xu et al. 2020), and relevant data are summarized in Table S2. Thus, the ionic type (particularly polyvalent cations) generally interacts with the key functional groups (especially oxygen-containing functional groups) in DBC, substantially influencing its aggregation behavior in aquatic systems.

The anion type also significantly influences the aggregation behavior of DBC. The CCC of DBC in SO_4^{2-} solutions is lower than that in Cl^- solutions, indicating that divalent anions induce a stronger aggregation tendency than monovalent anions (Yang et al. 2022). The anions and DBC particles share the same negative charge; therefore, their direct adsorption onto the surface is hindered. Consequently, the surface properties of both the particles and electrolytes play a crucial role in controlling DBC aggregation in anion-containing solutions. One contributing factor is that at equivalent concentrations, SO_4^{2-} exhibits significantly higher ionic strength than Cl^-, leading to a higher degree of compression of the electrical double layer around DBC in Na_2SO_4 solutions. This weakens the electrostatic repulsion and further promotes DBC particle aggregation (Li et al. 2021; Yang et al. 2022). Another key factor is that SO_4^{2-} (a kosmotropic anion) promotes intermolecular hydrogen-bonding network reorganization, thereby strengthening the hydrophobic interactions among the DBC particles and facilitating aggregation. In contrast, Cl^- (a chaotropic anion) disrupts hydrogen bonding between water molecules, destabilizing the hydrophobic interactions and suppressing aggregation (Chen et al. 2019; Moelbert et al. 2004). Thus, the ionic composition indirectly affects DBC particle aggregation by modulating intermolecular water interactions (Fig. 5).

4.2 pH

The aggregation behavior of DBC in aquatic systems is strongly pH dependent. The corresponding CCC_{Na} values of wheat-straw-derived DBC were 95.68, 107.86, and 128.89 mM at pH 5, 7, and 9, respectively, indicating enhanced aggregation under acidic conditions and improved colloidal stability under alkaline conditions (Tang et al. 2024). This pH dependence arises through multiple mechanisms. Under acidic conditions, the protonation of the surface functional groups (e.g., -OH and -COOH) reduces the surface charge and electrostatic repulsion, facilitating aggregation (Shao et al. 2021; Smith et al. 2008). Concurrently, an acidic pH alters polymer conformation, diminishes steric repulsion, and promotes deposition (Mierczynska-Vasilev and Beattie 2010). Under alkaline conditions, deprotonation increases the surface charge density and reduces the bond donors. The resulting enhanced hydration shell formation through DBC–water hydrogen bonding inhibits particle attachment (Tang et al. 2017). Additionally, alkaline conditions promote charge accumulation on polymer peripheries, potentially strengthening the hydrophobic interactions that resist destabilization (Li et al. 2018). Collectively, pH governs the aggregation and deposition processes of DBC by modulating the electrostatic forces, hydrogen bonding, steric effects, and hydrophobic interactions (Ou et al. 2021). These pH-dependent responses suggest that DBC colloidal stability may undergo significant alterations during pH fluctuations (e.g., acid mine drainage or acid rain events), or even within the common pH range (5–9), with profound implications for the environmental fate of both DBC and its associated contaminants (Tang et al. 2024).

4.3 Organic substances

Organic substances (including BSA and HA) mediate DBC aggregation through electrostatic interaction and steric effect, and the molecular weight of the organic substances exhibits a strong negative correlation with aggregation (Liu et al. 2024b). Increasing the molecular weight of organic substances enhances the thickness of the adsorption layer on the DBC surface, thereby strengthening the steric hindrance effects that inhibit aggregation and improve colloidal stability, ultimately

promoting DBC mobility in porous media (Yan et al. 2022). BSA adsorption on the DBC surface forms a protective corona layer that suppresses particle aggregation through steric stabilization (Li et al. 2024c; Yang et al. 2022). Notably, BSA enhances the colloidal stability of DBC more effectively in NaCl than in Na_2SO_4 solutions because of the greater negative surface charge and more complex three-dimensional structure of the adsorption layer in NaCl solutions, resulting in stronger electrostatic and steric repulsion (Gao et al. 2022). HA generally improves the colloidal stability of DBC in NaCl solutions (Li et al. 2024c) and preferentially adsorbs onto DBC surfaces, increasing their negative surface charge at neutral pH. This adsorption not only enhances the electrostatic repulsion between DBC particles (Dhangar et al. 2023; Gui et al. 2021) but also induces significant steric repulsion (Chekli et al. 2013; Yang et al. 2019). However, at high HA concentrations and elevated Ca^{2+} levels, Ca^{2+} bridging occurs between HA molecules and oxygen-containing functional groups on the DBC surface, leading to enhanced aggregation (Wang et al. 2013b; Xu et al. 2017).

Besides, the colloidal stability and consequent environmental mobility of DBC are significantly influenced by its coexisting environmental organic substances. For example, rice root exudates and low-molecular-weight organic acids (LMWOAs) are adsorbed onto DBC surfaces and induce colloidal destabilization. This effect is strongly dependent on the binding affinity between the LMWOAs and DBC surface functional groups (Gu et al. 2022; Lian et al. 2022). The adsorption process reduces the DBC surface potential, thereby diminishing the electrostatic repulsion forces and enhancing the aggregation propensity (Lian et al. 2022). In addition, antibiotics alter the transport behavior and fate of DBC. Under acidic to neutral conditions (pH 5–7), sulfamethazine and ciprofloxacin adsorption induces charge screening effects that decrease the DBC surface charge, ultimately reducing both the colloidal stability and soil mobility (Yang et al. 2020a; Zhao et al. 2021). Conversely, elevated pH significantly reduces DBC sorption to soil matrices through competitive retention and steric stabilization effects, leading to decreased co-transport efficiency of DBC and sulfamethazine in saturated soils (Liu et al. 2024a). These findings demonstrate that key environmental cofactors profoundly regulate DBC aggregation and transport behavior, ultimately governing the environmental fate of DBC and its associated contaminants.

4.4 Minerals

In aquatic systems, DBC frequently interacts with mineral surfaces through heteroaggregation, a distinct process from homoaggregation that involves the aggregation of dissimilar particles (Wang et al. 2015). This heteroaggregation is critically governed by the balance of attractive and repulsive forces between DBC functional groups and mineral sites. Depending on the respective surface properties, these interactions can either promote aggregation via charge neutralization or bridging, or enhance stability by increasing electrostatic repulsion (Gui et al. 2021; Liu et al. 2022a; Yan et al. 2022). Kaolinite, a negatively charged mineral, enhances the colloidal stability of DBC by increasing electrostatic repulsion through surface interactions, thereby promoting its mobility in porous media (Yan et al. 2022). In contrast, wheat-straw-derived DBC exhibits accelerated aggregation in the presence of kaolinite owing to hydroxyl and carboxyl group interactions, which induce charge screening and reduce electrostatic repulsion, ultimately promoting destabilization (Gui et al. 2021). Under neutral pH conditions, goethite and hematite markedly decrease the colloidal stability of DBC through electrostatic attraction, suppressing its environmental mobility (Lian et al. 2019). The needle-like structure of goethite provides more adsorption sites than that of hematite, resulting in stronger heteroaggregation and faster aggregation of DBC (Yan et al. 2022). However, manure-derived DBC displays an increased CCC and undergoes slower aggregation in the presence of goethite. This is likely because goethite forms a surface coating on the manure-derived DBC, where the resulting electrostatic shielding and steric hindrance override the attractive forces, thereby inhibiting particle destabilization (Gui et al. 2021). This highlights that the surface properties of DBC are a critical factor determining the mineral-DBC interactions.

4.5 Aging

The aging of DBC in aquatic systems encompasses primarily photoaging and chemical aging. Photoaging mediates structural transformations in DBC that directly govern its colloidal stability (Tang et al. 2024; Xu et al. 2017). UV irradiation induces a three-stage transformation process in DBC involving photodecarboxylation, photooxidation, and mineral exposure, with a reduced Hamaker constant, suggesting increased colloidal stability of aged DBC (Tang et al. 2024). Photoaging induces aromatic oxidation and carboxyl group formation of DBC, thereby modifying its surface properties and potentially enhancing its colloidal stability in $CaCl_2$ solutions. Concurrently, increased oxygen-containing functional groups elevate surface charge, further strengthening stabilization via combined electrostatic and hydration forces (Xu et al. 2017). In addition to photoaging, the environmental transport of DBC is modulated by chemical aging, which significantly alters its aggregation behavior (Wang et al. 2019; Yang et al. 2024; Zhao and Shang 2023). Nitric-acid-oxidized DBC exhibits a substantial increase

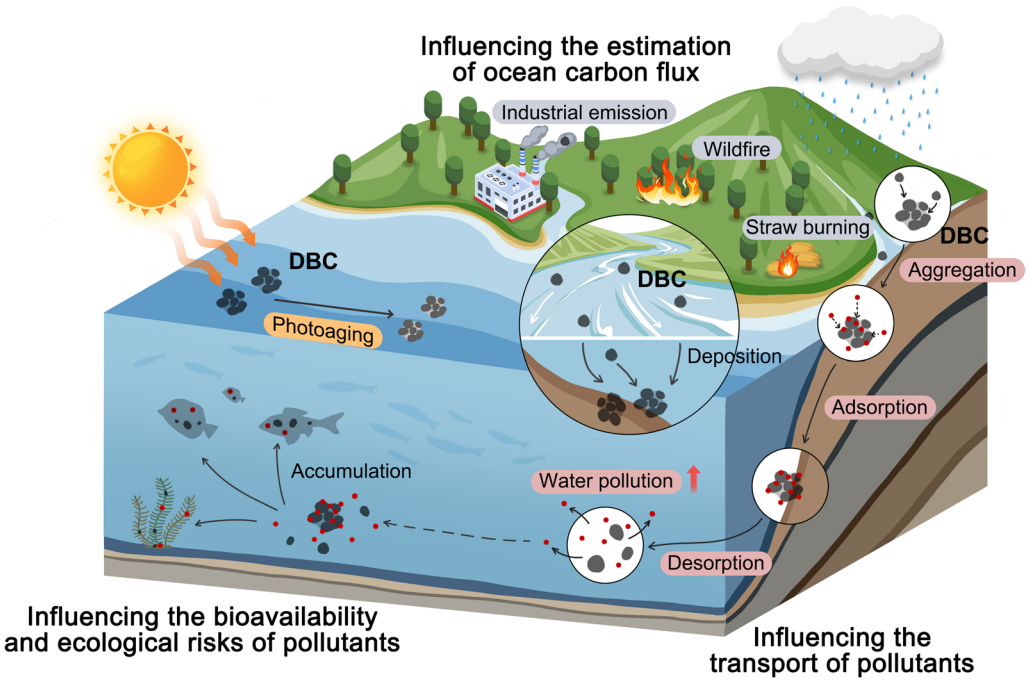

Fig. 6 Schematic diagram to illustrate the environmental implications of DBC colloidal stability, including the impacts on biogeochemical processes in terrestrial/aquatic systems, the transport and environmental fate of associated pollutants, and marine carbon flux estimation of DBC

in negatively charged carboxyl groups, leading to a higher CCC in NaCl solutions. Conversely, the CCC decreases in $CaCl_2$ solutions, probably resulting from greater surface charge neutralization and Ca^{2+} bridging (Wang et al. 2019). Aged DBC exhibits greater mobility in water-saturated porous media under environmentally relevant conditions, which is attributed to its higher hydrophilicity, increased surface roughness, and reduced particle size (Yang et al. 2024; Zhao and Shang 2023). These findings suggest that aging processes diminish the aggregation potential of DBC in aquatic systems while promoting environmental mobility (Wang et al. 2019).

5 Environmental implications of the colloidal stability of DBC

5.1 Influencing the structural form and utilization of DBC in soil and water bodies

The aggregation of DBC leads to the formation of larger particulate matter, which significantly alters environmental speciation in aquatic systems. Notably, the speciation of DBC (e.g., dissolved or particulate phases) critically governs its environmental applications and pollutant bioavailability, thereby influencing ecological risks in both terrestrial and aquatic ecosystems (Fig. 6). DBC strongly interacts with microbial communities through direct aggregation and surface reactions, which play pivotal roles in the regulation of microbial activity, extracellular electron transfer, functional performance, and nutrient cycling efficiency (Yang et al. 2020b; Yuan et al. 2025). Although DBC can be absorbed by the root systems of plants and transported to aboveground tissues (Li et al. 2023b), its particle size enlargement induced by aggregation may decrease plant uptake efficiency. Furthermore, DBC demonstrates remarkable capabilities for facilitating nanoplastic aggregation and sedimentation(Xu et al. 2021). Particulate-phase DBC adsorbs nanoplastic and creates a barrier effect, effectively reducing nanoplastic bioavailability and significantly alleviating oxidative stress in lettuce roots and shoots, thereby mitigating nanoplastic phytotoxicity (Shen et al. 2023; Xia et al. 2023; Yu and Li 2024). It is also noteworthy that DBC can mediate the generation of reactive oxygen species (ROS) in environmental matrices, affecting microbial community composition, nutrient element release, and the conversion of multivalent metals (Yao et al. 2025). Moreover, the colloidal stability of DBC governs its environmental persistence and dispersion, thereby modulating the spatial and temporal scales of ROS-mediated effects. This represents another significant pathway for DBC to influence biogeochemical cycles and mediate the transformation of coexisting pollutants. These findings highlight the need to focus on DBC aggregation, which modulates the bioavailability of both DBC itself and coexisting pollutants in environmental systems.

5.2 Influencing the transport of pollutants and their environmental fate

DBC is characterized by high aromaticity, small molecular dimensions, and abundant oxygen-containing functional groups (Li et al. 2024a; Qu et al. 2016; Tang et al. 2024). The aromatic domains and oxygen-containing functional moieties in DBC act as critical binding sites for organic pollutants and heavy metals, while also influencing the pollutant transformation pathways. Consequently, as a highly reactive environmental mediator, the colloidal behavior of DBC governs the distribution and transport of the associated pollutants. The presence of heavy metal cations (e.g., Cu^{2+}, Cd^{2+}, Ni^{2+}, and Pb^{2+}) significantly promotes DBC aggregation via strong complexation and cation-π interactions (Huang et al. 2021; Song et al. 2021; Xu et al. 2020). Metal-complexed DBC undergoes pronounced sedimentation, thus facilitating the co-transport of heavy metals and their subsequent concentration in sediments. This not only poses a long-term threat to sediment-dwelling organisms but also raises concerns about the biomagnification potential of these bioavailable heavy metals (Fig. 6). Although DBC facilitates the mobility of organic pollutants in porous media, the process is largely regulated by aggregation. For instance, the adsorption of bisphenol A (BPA) on DBC is highly dependent on the available surface sites. Aggregation reduces the number of accessible sorption sites and encapsulates functional groups within DBC aggregates, thereby diminishing the BPA adsorption capacity and altering its transport behavior (Xing et al. 2023). Moreover, DBC mediates the decomposition of antibiotic resistance genes (ARGs) in aquatic systems, primarily through hydroxyl radical (·OH) generation—a process strongly correlated with its molecular size (Lian et al. 2020). Aggregation-induced changes in the particle size distribution of DBC may profoundly influence the environmental fate of contaminants, particularly large-molecular-weight organics such as ARGs. Furthermore, aging processes (e.g., photoaging) reduce the surface area and reactive sites of DBC, thereby modulating the aggregation behavior (Jiang et al. 2023; Li et al. 2023a; Wang et al. 2022). Notably, sunlight-induced radicals from DBC not only degrade the adsorbed pollutants but may also destabilize DBC itself, potentially releasing sequestered pollutants back into aquatic environments and increasing the secondary contamination potential (Tang et al. 2024; Zhang et al. 2022). Consequently, enhanced colloidal stability of DBC may facilitate the long-range co-transport of pollutants and broaden their spatial exposure scope, while decreased stability promotes the aggregation and deposition of both DBC and associated pollutants, thereby shifting the primary exposure route from the water column to benthic sediments. This shift creates localized contamination hotspots, increases exposure for sediment-dwelling communities, and may alter long-term leaching behavior.

5.3 Influencing the estimation of ocean carbon flux

During fluvial transport to estuarine systems, DBC undergoes aggregation-mediated conversion to particulate matter, which is ultimately deposited in sediments, consequently reducing its vertical flux in estuarine zones (Qi et al. 2020; Xu et al. 2017). Similar flux attenuation phenomena have been documented in freshwater systems (Xu et al. 2017). Terrestrial-derived DBC predominantly discharges into marine environments, which represent the ultimate global sink with an estimated annual accumulation of ~27 Tg C $year^{-1}$ (Jaffé et al. 2013; Zhou et al. 2024). Critically, in estuarine mixing zones where ionic strength is elevated, specific cations such as Ca^{2+} and Ba^{2+} reduce the energy barrier between DBC particles through complexation and charge screening, thereby promoting the aggregation of DBC particles. Consequently, the aggregation behavior of DBC, coupled with its sorption affinity for assorted pollutants, may result in their co-deposition into estuarine sediments. Therefore, a substantial fraction of terrestrially sourced DBC and its associated pollutants may be sequestered in riverine and estuarine sediments through aggregation-deposition processes, effectively removing these constituents from the DOM pool (Fig. 6). Sedimentary trapping prevents subsequent transport to oceanic systems. Concurrently, photochemical aging induced by solar radiation further modifies the environmental behavior of DBC (Tang et al. 2024; Wang et al. 2023a). The DBC/DOM ratio has been conventionally employed as a conservative tracer to estimate global DBC fluxes (Jaffé et al. 2013; Stubbins et al. 2015). However, the aggregation behavior of DBC reveals that this ratio demonstrates progressive depletion along salinity gradients owing to DBC fractionation processes, potentially leading to systematic overestimation of the land-to-ocean DBC flux when using this metric (Hu et al. 2024; Xu et al. 2017).

6 Conclusions and future prospects

6.1 Conclusions

DBC exhibits complex colloidal behaviors, including aggregation, sedimentation, and surface interactions, which critically govern the environmental fate and mobility of the associated pollutants in aquatic systems. The aggregation of DBC is fundamentally controlled by its molecular architecture and surface chemistry, which in turn depend on the biomass sources, pyrolysis conditions, and environmental parameters. Theoretical frameworks (DLVO/XDLVO) identified electrostatic and Lewis AB interactions as the dominant forces driving

the unique aggregation behavior of DBC, distinguishing it from conventional dissolved organic matter. Environmental variables, such as the ionic composition, pH, organic substances, mineral surfaces, and aging processes, collectively modulated these interactions. These colloidal behaviors directly influence the environmental persistence of DBC, the pollutant carrier effects, and the ultimate role in global carbon cycling through modified land-to-ocean carbon fluxes. Nevertheless, it should be noted that certain mechanistic insights into specific interactions and colloidal behavior of DBC are currently derived from experimental conditions with inherent limitations and uncertainties, which need further investigation at multiple scales and should be addressed in future research.

6.2 Future prospects

Research on the colloidal stability of DBC has made significant progress. Nevertheless, this understanding still faces persistent knowledge gaps that hinder predictive capability and accurate risk assessment in complex environments. A primary limitation is the absence of standardized molecular characterization protocols for DBC. While the heterogeneity of DBC is well-recognized, the lack of consistent molecular-level analytical procedures across studies severely compromises the comparability of published data. In addition, the mechanistic insights into contaminant-mediated heteroaggregation of DBC remain limited. Most studies have focused on homoaggregation of DBC or its adsorption capacity for pollutants in isolation. While pollutant adsorption alters DBC surface properties and thereby modifies subsequent heteroaggregation and co-transport, this interdependent process remains poorly quantified. Furthermore, there is still a lack of robust predictive models for the colloidal stability of DBC in natural aquatic systems. Current approaches relying on conventional metrics often fail to adequately account for the complexity of environmental conditions, resulting in significant uncertainty when forecasting the large-scale transport and sequestration of DBC and associated pollutants. Collectively, addressing these limitations is crucial for bridging the critical knowledge gaps.

Future research should prioritize the integration of advanced analytical techniques (e.g., FT-ICR-MS coupled with multidimensional NMR spectroscopy) to establish universally comparable structural fingerprints. This foundational work is essential for linking the source, structure, and function of DBC. Simultaneously, the current understanding of DBC heteroaggregation with coexisting nanomaterials and pollutants remains incomplete, with most studies focusing primarily on the inherent aggregation behavior of DBC and pollutant adsorption properties. Deeper mechanistic investigations should examine the synchronous changes in DBC heteroaggregation during pollutant adsorption, particularly surface structural modifications. Establishing the relationships between key structural transformations and colloidal stability will significantly improve the prediction of DBC and the associated pollutant transport, distribution, and environmental fate in complex systems. Current approaches that rely on CCC measurements lack the robustness required for comprehensive behavioral forecasting. Given that the colloidal stability of DBC is governed by both its structural characteristics and environmental conditions, emerging artificial intelligence techniques offer transformative potential. By integrating molecular characterization data with environmental parameters using machine-learning algorithms, researchers can identify the dominant aggregation-influencing factors and develop reliable predictive models. Such advanced methodologies are particularly valuable for optimizing water treatment efficiency and accurately assessing pollutant risks. Future efforts should prioritize the development of practical prediction tools capable of evaluating the colloidal stability of DBC across diverse environmental scenarios.

Supplementary Information

The online version contains supplementary material available at https://doi.org/10.1007/s42773-026-00627-7.

Additional file 1.

Acknowledgements

This work was supported by the National Natural Science Foundation of China (Grant Nos. 42307489, 42377383 and 22206132), State Key Laboratory of Water Pollution Control and Green Resource Recycling Foundation (Grant No. PCRRF25042), the Natural Science Foundation of Jiangsu Province (Grants No. BK20230764) and Fundamental Research Project of Yunnan Province (Grant No. 202201AT070773). We also thank the three anonymous reviewers for their critical reading and helpful comments, which significantly strengthened the mechanistic interpretation and overall quality of this manuscript.

Author contributions

Fanchao Xu: Conceptualisation, Writing–original draft, Investigation, Funding acquisition, Writing—Review & Editing. Jun Zhu: Visualization, Investigation, Data curation. Kun Liu: Writing–review & editing, Supervision, Resources, Funding acquisition. Minli Wang: Investigation, Methodology, Funding acquisition. Huiting Liu: Investigation, Formal analysis, Funding acquisition. Jianjun Lian: Writing–review & editing, Resources, Data curation. Xiaolei Qu: Writing–review & editing, Resources, Funding acquisition. Bingyu Wang: Writing–review & editing, Supervision, Project administration, Methodology. All authors read and approved the final manuscript.

Funding

This work was funded by National Natural Science Foundation of China (42307489, Fanchao Xu, 42377383, Xiaolei Qu, 22206132, Huiting Liu), State Key Laboratory of Water Pollution Control and Green Resource Recycling Foundation (PCRRF25042, Fanchao Xu), Natural Science Foundation of Jiangsu Province (BK20230764, Kun Liu), Fundamental Research Project of Yunnan Province (202201AT070773, Minli Wang).

Data availability

This article is a review and does not report new primary data. All data discussed are extracted from previously published studies cited in the

manuscript. Any compiled datasets generated during the current study are available from the corresponding author upon reasonable request.

Declarations

Competing interests

The authors declare that they have no known competing financial interests or personal relationships that could have appeared to influence the work reported in this paper.

Author details

[1]School of Energy and Environment, Anhui University of Technology, Maanshan 243002, China. [2]State Key Laboratory of Water Pollution Control and Green Resource Recycling, School of Environment, Nanjing University, Nanjing 210023, China. [3]Key Laboratory of Environmental Remediation and Ecological Health (Ministry of Industry and Information Technology), Jiangsu Environmental Engineering Technology Co., Ltd., Nanjing 210019, China. [4]Faculty of Civil Engineering and Mechanics, Kunming University of Science and Technology, Kunming 650500, China. [5]School of Environmental and Chemical Engineering, Shenyang Ligong University, Shenyang 110159, China. [6]School of Environmental and Biological Engineering, Nanjing University of Science and Technology, Nanjing 210094, China.

Received: 29 October 2025 Revised: 26 March 2026 Accepted: 26 April 2026
Published online: 11 June 2026

References

Azeredo J, Visser J, Oliveira R (1999) Exopolymers in bacterial adhesion: interpretation in terms of DLVO and XDLVO theories. Colloids Surf B Biointerfaces 14(1–4):141–148

Bao H, Niggemann J, Luo L, Dittmar T, Kao SJ (2017) Aerosols as a source of dissolved black carbon to the ocean. Nat Commun 8(1):510

Chang Z, Tian L, Li F, Wu M, Steinberg CEW, Pan B, Xing B (2020) Organo-mineral complexes protect condensed organic matter as revealed by benzene-polycarboxylic acids. Environ Pollut 260:113977

Chekli L, Phuntsho S, Roy M, Shon HK (2013) Characterisation of Fe-oxide nanoparticles coated with humic acid and Suwannee River natural organic matter. Sci Total Environ 461–462:19–27

Chen KL, Elimelech M (2009) Relating colloidal stability of fullerene (C_{60}) nanoparticles to nanoparticle charge and electrokinetic properties. Environ Sci Technol 43(19):7270–7276

Chen W, Li D, Bu Y, Chen G, Wan X, Li N (2019) Design of strong and tough methylcellulose-based hydrogels using kosmotropic Hofmeister salts. Cellulose 27(3):1113–1126

Chen Q, Ma Y, Dong J, Kong Y, Wu M (2022a) The chemical structure characteristics of dissolved black carbon and their binding with phenanthrene. Chemosphere 291:132747

Chen Y, Sun K, Wang Z, Zhang E, Yang Y, Xing B (2022b) Analytical methods, molecular structures and biogeochemical behaviors of dissolved black carbon. Carbon Res 1(1):23

Coppola AI, Wagner S, Lennartz ST, Seidel M, Ward ND, Dittmar T, Santín C, Jones MW (2022) The black carbon cycle and its role in the Earth system. Nat Rev Earth Env 3(8):516–532

Dhangar K, Kumar M, Aouad M, Mahlknecht J, Raval NP (2023) Aggregation behaviour of black carbon in aquatic solution: effect of ionic strength and coexisting metals. Chemosphere 311(2):137088

Du Z, Hu A, Wang Q, Ai J, Zhang W, Liang Y, Cao M, Wu H, Wang D (2022) Molecular composition and biotoxicity effects of dissolved organic matters in sludge-based carbon: effects of pyrolysis temperature. J Hazard Mater 424:127346

Eckhardt S, Pisso I, Evangeliou N, Zwaaftink CG, Plach A, McConnell JR, Sigl M, Ruppel M, Zdanowicz C, Lim S, Chellman N, Opel T, Meyer H, Steffensen JP, Schwikowski M, Stohl A (2023) Revised historical Northern Hemisphere black carbon emissions based on inverse modeling of ice core records. Nat Commun 14(1):271

Fan L, Han T, Huang X, Zhang Y, Zhai W, Zhang D, Pan X (2025) Contradictions in dissolved black carbon research: a critical review of its sources, structures, analytical methods, and environmental behaviors. Environ Pollut 374:126276

Fang J, Cheng L, Hameed R, Jin L, Wang D, Owens G, Lin D (2020) Release and stability of water dispersible biochar colloids in aquatic environments: effects of pyrolysis temperature, particle size, and solution chemistry. Environ Pollut 260:114037

Fang J, Jin L, Meng Q, Shan S, Wang D, Lin D (2022) Biochar effectively inhibits the horizontal transfer of antibiotic resistance genes via transformation. J Hazard Mater 423:127150

Fang Y, Huang G, Liu D, Wu M, Wang Y, He J, Chen C, Lin T, Yang S, Chen Y (2025) Differential nonconservative behaviors of dissolved black carbon along a major river-estuary-shelf continuum. J Geophys Res Oceans 130(6):e2025JC022432

Fu H, Liu H, Mao J, Chu W, Li Q, Alvarez PJJ, Qu X, Zhu D (2016) Photochemistry of dissolved black carbon released from biochar: reactive oxygen species generation and phototransformation. Environ Sci Technol 50(3):1218–1226

Fu H, Liu K, Alvarez PJJ, Yin D, Qu X, Zhu D (2019) Quantifying hydrophobicity of natural organic matter using partition coefficients in aqueous two-phase systems. Chemosphere 218:922–929

Gao Y, Zeng X, Zhang W, Zhou L, Xue W, Tang M, Sun S (2022) The aggregation behaviour and mechanism of commercial graphene oxide in surface aquatic environments. Sci Total Environ 806(4):150942

Garnett J, Halsall C, Thomas M, Crabeck O, France J, Joerss H, Ebinghaus R, Kaiser J, Leeson A, Wynn PM (2021) Investigating the uptake and fate of poly- and perfluoroalkylated substances (PFAS) in sea ice using an experimental sea ice chamber. Environ Sci Technol 55(14):9601–9608

Gu S, Lian F, Han Y, Wang Z, Xing B (2022) Effect of root exudates on the release, surface property, colloidal stability, and phytotoxicity of dissolved black carbon. Ecotoxicol Environ Saf 239:113687

Gui X, Liu C, Li F, Wang J (2020) Effect of pyrolysis temperature on the composition of DOM in manure-derived biochar. Ecotoxicol Environ Saf 197:110597

Gui X, Song B, Chen M, Xu X, Ren Z, Li X, Cao X (2021) Soil colloids affect the aggregation and stability of biochar colloids. Sci Total Environ 771:145414

Hameed R, Li G, Son Y, Fang H, Kim T, Zhu C, Feng Y, Zhang L, Abbas A, Zhao X, Wang J, Li J, Dai Z, Du D (2023) Structural characteristics of dissolved black carbon and its interactions with organic and inorganic contaminants: a critical review. Sci Total Environ 872:162210

Han L, Nie X, Wei J, Gu M, Wu W, Chen M (2021) Effects of feedstock biopolymer compositions on the physiochemical characteristics of dissolved black carbon from lignocellulose-based biochar. Sci Total Environ 751:141491

Hao Y, Ma C, Cai Z, Han L, Jia W, Cao Y, White JC, Liang A, Xu X, Li H, Chen G, Xiao J, Zheng W, Pagano L, Maestri E, Marmiroli M, Marmiroli N, Zhao J, Xing B (2025) Safe production of rice (*Oryza sativa* L.) in arsenic-contaminated soil: a remedial strategy using micro-nanostructured bone biochar. Environ Sci Technol 59(7):3666–3678

He H, Liu J, Shu Z, Chen Y, Pan Z, Peng C, Wang X, Zhou F, Zhou M, Du Z, Sun K, Xing B, Wang Z (2024) Microbially driven iron cycling facilitates organic carbon accrual in decadal biochar-amended soil. Environ Sci Technol 58(28):12430–12440

Hu A, Zheng Y, Wang Z, Li M, Wang D, Zhang W (2023) Tracking the transformation pathway of dissolved organic matters (DOMs) in biochars under sludge pyrolysis via reactomics and molecular network analysis. Chemosphere 342:140149

Hu A, Jang KS, Tanentzap AJ, Zhao W, Lennon JT, Liu J, Li M, Stegen J, Choi M, Lu Y, Feng X, Wang J (2024) Thermal responses of dissolved organic matter under global change. Nat Commun 15(1):576

Hu J, Liu CG, Zhang WK, Liu XW, Dong B, Wang ZD, Xie YG, Hua ZS, Liu XW (2025) Decomposing the molecular complexity and transformation of dissolved organic matter for innovative anaerobic bioprocessing. Nat Commun 16(1):4859

Huang M, Li Z, Wen J, Ding X, Zhou M, Cai C, Shen F (2021) Molecular insights into the effects of pyrolysis temperature on composition and copper binding properties of biochar-derived dissolved organic matter. J Hazard Mater 410:124537

Jaffé R, Ding Y, Niggemann J, Vähätalo AV, Stubbins A, Spencer RGM, Campbell J, Dittmar T (2013) Global charcoal mobilization from soils via dissolution and riverine transport to the oceans. Science 340(6130):345–347

Jamieson T, Sager E, Guéguen C (2014) Characterization of biochar-derived dissolved organic matter using UV–visible absorption and excitation–emission fluorescence spectroscopies. Chemosphere 103:197–204
Ji R, Yang Y, Wu Y, Zhu C, Min J, Liu C, Zhang L, Cheng H, Xue J, Zhou D (2024) Capturing differences in the release potential of dissolved organic matter from biochar and hydrochar: insights from component characterization and molecular identification. Sci Total Environ 955:177209
Jiang M, He L, Niazi NK, Wang H, Gustave W, Vithanage M, Geng K, Shang H, Zhang X, Wang Z (2023) Nanobiochar for the remediation of contaminated soil and water: challenges and opportunities. Biochar 5(1):2
Kim HB, Kim JG, Kim T, Alessi DS, Baek K (2020) Mobility of arsenic in soil amended with biochar derived from biomass with different lignin contents: relationships between lignin content and dissolved organic matter leaching. Chem Eng J 393:124687
Kloster N, Brigante M, Zanini G, Avena M (2013) Aggregation kinetics of humic acids in the presence of calcium ions. Colloid Surface A 427:76–82
Li M, Zhang A, Wu H, Liu H, Lv J (2017) Predicting potential release of dissolved organic matter from biochars derived from agricultural residues using fluorescence and ultraviolet absorbance. J Hazard Mater 334:86–92
Li W, Liao P, Oldham T, Jiang Y, Pan C, Yuan S, Fortner JD (2018) Real-time evaluation of natural organic matter deposition processes onto model environmental surfaces. Water Res 129:231–239
Li X, He E, Jiang K, Peijnenburg WJGM, Qiu H (2021) The crucial role of a protein corona in determining the aggregation kinetics and colloidal stability of polystyrene nanoplastics. Water Res 190:116742
Li Q, Zhang X, Mao M, Wang X, Shang J (2023a) Carbon content determines the aggregation of biochar colloids from various feedstocks. Sci Total Environ 880:163313
Li Y, Ge C, Cheng C, Wang X, Si D, Mu C, Wang M, Li H, Zhou D (2023b) Nanobiochar uptake and translocation by plants: assessing environmental fate and food chain risk. Sci Total Environ 905:167012
Li L, Cheng W, Xie X, Zhao R, Wang Y, Wang Z (2024a) Photo-reactivity of dissolved black carbon unveiled by combination of optical spectroscopy and FT-ICR MS analysis: effects of pyrolysis temperature. Water Res 251:121138
Li L, Wei B, Cheng W, Kang Y, Xie X, Wang Z (2024b) Dual role of dissolved black carbon in sensitized ofloxacin photooxidation: mechanism and influential factors. Sci Total Environ 944:173969
Li Q, Si H, Chen X, Mao M, Shang J (2024c) Influence of natural organic matter on the aggregation dynamics of biochar colloids derived from various feedstocks. Sci Total Environ 946:174097
Li X, Tan M, Wu B, Wang J, Ma J, Chen B, Chu C (2024d) Redox oscillation-driven production of reactive oxygen species from black carbon. Environ Sci Technol 58(48):21210–21217
Lian F, Xing B (2017) Black carbon (biochar) in water/soil environments: molecular structure, sorption, stability, and potential risk. Environ Sci Technol 51(23):13517–13532
Lian F, Xing B (2024) From bulk to nano: formation, features, and functions of nano-black carbon in biogeochemical processes. Environ Sci Technol 58(36):15910–15925
Lian F, Yu W, Wang Z, Xing B (2019) New insights into black carbon nanoparticle-induced dispersibility of goethite colloids and configuration-dependent sorption for phenanthrene. Environ Sci Technol 53(2):661–670
Lian F, Yu W, Zhou Q, Gu S, Wang Z, Xing B (2020) Size matters: nano-biochar triggers decomposition and transformation inhibition of antibiotic resistance genes in aqueous environments. Environ Sci Technol 54(14):8821–8829
Lian F, Gu S, Han Y, Wang Z, Xing B (2022) Novel insights into the impact of nano-biochar on composition and structural transformation of mineral/nano-biochar heteroaggregates in the presence of root exudates. Environ Sci Technol 56(13):9816–9825
Liu G, Zheng H, Jiang Z, Zhao J, Wang Z, Pan B, Xing B (2018) Formation and physicochemical characteristics of nano biochar: insight into chemical and colloidal stability. Environ Sci Technol 52(18):10369–10379
Liu CH, Chu W, Li H, Boyd SA, Teppen BJ, Mao J, Lehmann J, Zhang W (2019a) Quantification and characterization of dissolved organic carbon from biochars. Geoderma 335:161–169
Liu K, Fu H, Zhu D, Qu X (2019b) Prediction of apolar compound sorption to aquatic natural organic matter accounting for natural organic matter hydrophobicity using aqueous two-phase systems. Environ Sci Technol 53(14):8127–8135
Liu Y, Ma J, Gao J, Chen X, Ouyang X, Weng L, Li H, Chen Y, Li Y (2022a) Stability and interaction of biochar and iron mineral nanoparticles: effect of pH, ionic strength, and dissolved organic matter. Biochar 4(1):47
Liu Y, Wang M, Yin S, Xie L, Qu X, Fu H, Shi Q, Zhou F, Xu F, Tao S, Zhu D (2022b) Comparing photoactivities of dissolved organic matter released from rice straw-pyrolyzed biochar and composted rice straw. Environ Sci Technol 56(4):2803–2815
Liu M, Liu X, Hu Y, Zhang Q, Farooq U, Qi Z, Lu L (2024a) Mobility of biochar-derived dissolved organic matter and its effects on sulfamerazine transport through saturated soil porous media. Environ Sci-Processes Impacts 26(12):2264–2278
Liu M, Lu Q, Graham N, Yu W (2024b) The influence of molecular weight of adsorbed natural organic matter on the removal of dissolved black carbon by coagulation. Chem Eng J 488:151097
Lu Q, Han Q, Liu H, Feng L, Liu Y, Du Z, Zhang L (2024) Molecular-level transformations of dissolved black carbon in UV-based advanced oxidation processes. Water Res 260:121962
Mierczynska-Vasilev A, Beattie DA (2010) Adsorption of tailored carboxymethyl cellulose polymers on talc and chalcopyrite: correlation between coverage, wettability, and flotation. Miner Eng 23(11–13):985–993
Moelbert S, Normand B, De Los Rios P (2004) Kosmotropes and chaotropes: modelling preferential exclusion, binding and aggregate stability. Biophys Chem 112(1):45–57
Mohona TM, Gupta A, Masud A, Chien SC, Lin LC, Nalam PC, Aich N (2019) Aggregation behavior of inorganic 2D nanomaterials beyond graphene: insights from molecular modeling and modified DLVO theory. Environ Sci Technol 53(8):4161–4172
Mukherjee A, Zimmerman AR (2013) Organic carbon and nutrient release from a range of laboratory-produced biochars and biochar–soil mixtures. Geoderma 193–194:122–130
Ou Q, Xu Y, He Q, Wu Z, Ma J, Huangfu X (2021) Deposition behavior of dissolved black carbon on representative surfaces: role of molecular conformation. J Environ Chem Eng 9(5):105921
Qi Y, Fu W, Tian J, Luo C, Shan S, Sun S, Ren P, Zhang H, Liu J, Zhang X, Wang X (2020) Dissolved black carbon is not likely a significant refractory organic carbon pool in rivers and oceans. Nat Commun 11(1):5051
Qu X, Fu H, Mao J, Ran Y, Zhang D, Zhu D (2016) Chemical and structural properties of dissolved black carbon released from biochars. Carbon 96:759–767
Rajapaksha AU, Ok YS, El-Naggar A, Kim H, Song F, Kang S, Tsang YF (2019) Dissolved organic matter characterization of biochars produced from different feedstock materials. J Environ Manage 233:393–399
Roebuck JA, Seidel M, Dittmar T, Jaffé R (2018) Land use controls on the spatial variability of dissolved black carbon in a subtropical watershed. Environ Sci Technol 52(15):8104–8114
Seelen E, Liem-Nguyen V, Wunsch U, Baumann Z, Mason R, Skyllberg U, Bjorn E (2023) Dissolved organic matter thiol concentrations determine methylmercury bioavailability across the terrestrial-marine aquatic continuum. Nat Commun 14(1):6728
Shao Z, Luo S, Liang M, Ning Z, Sun W, Zhu Y, Mo J, Li Y, Huang W, Chen C (2021) Colloidal stability of nanosized activated carbon in aquatic systems: effects of pH, electrolytes, and macromolecules. Water Res 203:117561
Shen M, Liu S, Hu T, Zheng K, Wang Y, Long H (2023) Recent advances in the research on effects of micro/nanoplastics on carbon conversion and carbon cycle: a review. J Environ Manage 334:117529
Smith B, Wepasnick K, Schrote KE, Bertele AR, Ball WP, O'Melia C, Fairbrother DH (2008) Colloidal properties of aqueous suspensions of acid-treated, multi-walled carbon nanotubes. Environ Sci Technol 43(3):819–825
Song B, Chen M, Zhao L, Qiu H, Cao X (2019) Physicochemical property and colloidal stability of micron- and nano-particle biochar derived from a variety of feedstock sources. Sci Total Environ 661:685–695
Song C, Shan S, Yang C, Zhang C, Zhou X, Ma Q, Yrjälä K, Zheng H, Cao Y (2020) The comparison of dissolved organic matter in hydrochars and biochars from pig manure. Sci Total Environ 720:137423
Song F, Li T, Shi Q, Guo F, Bai Y, Wu F, Xing B (2021) Novel insights into the molecular-level mechanism linking the chemical diversity and copper binding heterogeneity of biochar-derived dissolved black carbon and dissolved organic matter. Environ Sci Technol 55(17):11624–11636

Song F, Li T, Wu F, Leung KMY, Hur J, Zhou L, Bai Y, Zhao X, He W, Ruan M (2023) Temperature-dependent molecular evolution of biochar-derived dissolved black carbon and its interaction mechanism with polyvinyl chloride microplastics. Environ Sci Technol 57(18):7285–7297
Stubbins A, Spencer RGM, Mann PJ, Holmes RM, McClelland JW, Niggemann J, Dittmar T (2015) Utilizing colored dissolved organic matter to derive dissolved black carbon export by Arctic rivers. Front Earth Sci 3:63
Sun Y, Xiong X, He M, Xu Z, Hou D, Zhang W, Ok YS, Rinklebe J, Wang L, Tsang DCW (2021) Roles of biochar-derived dissolved organic matter in soil amendment and environmental remediation: A critical review. Chem Eng J 424:130387
Sun L, Wang T, Li B, Wu J, Liu L, Liu J, Liu S, Wu P, Li Y, Dang Z, Zhu N (2025) Molecular fractionation during coprecipitation of dissolved black carbon with Fe(III): Preferential carbon sequestration for redox active molecules. Chem Eng J 505:159238
Taherymoosavi S, Joseph S, Pace B, Munroe P (2018) A comparison between the characteristics of single- and mixed-feedstock biochars generated from wheat straw and basalt. J Anal Appl Pyrol 129:123–133
Tang H, Zhao Y, Yang X, Liu D, Shao P, Zhu Z, Shan S, Cui F, Xing B (2017) New insight into the aggregation of graphene oxide using molecular dynamics simulations and extended Derjaguin–Landau–Verwey–Overbeek Theory. Environ Sci Technol 51(17):9674–9682
Tang N, Guo Y, Zhu Z, Jiang L, Li N, Hu T, Lu L, Zhang J, Li X, Liang J (2024) New insights into aggregation behaviors of the UV-irradiated dissolved biochars (DBioCs) in aqueous environments: effects of water chemistries and variation in the Hamaker constant. Environ Sci Technol 58(18):8053–8064
van Oss CJ (1995) Hydrophobicity of biosurfaces—origin, quantitative determination and interaction energies. Colloids Surf B Biointerfaces 5(3–4):91–110
van Oss CJ (2003) Long-range and short-range mechanisms of hydrophobic attraction and hydrophilic repulsion in specific and aspecific interactions. J Mol Recognit 16(4):177–190
Van Oss CJ (2006) Interfacial forces in aqueous media. CRC press
Wang D, Zhang W, Hao X, Zhou D (2013a) Transport of biochar particles in saturated granular media: effects of pyrolysis temperature and particle size. Environ Sci Technol 47(2):821–828
Wang LF, Wang LL, Ye XD, Li WW, Ren XM, Sheng GP, Yu HQ, Wang XK (2013b) Coagulation kinetics of humic aggregates in mono- and di-valent electrolyte solutions. Environ Sci Technol 47(10):5042–5049
Wang H, Adeleye AS, Huang Y, Li F, Keller AA (2015) Heteroaggregation of nanoparticles with biocolloids and geocolloids. Adv Colloid Interface Sci 226:24–36
Wang Y, Zhang W, Shang J, Shen C, Joseph SD (2019) Chemical aging changed aggregation kinetics and transport of biochar colloids. Environ Sci Technol 53(14):8136–8146
Wang H, Zhou H, Ma J, Nie J, Yan S, Song W (2020) Triplet photochemistry of dissolved black carbon and its effects on the photochemical formation of reactive oxygen species. Environ Sci Technol 54(8):4903–4911
Wang Y, Wang C, Xiong J, Zhang Q, Shang J (2022) Effects of low molecular weight organic acids on aggregation behavior of biochar colloids at acid and neutral conditions. Biochar 4(1):20
Wang L, Li J, Zhao J, Li H, Feng J, Zhang P, Pan B (2023a) Photodegradation of clindamycin by the dissolved black carbon is simultaneously regulated by ROS generation and the binding effect. Water Res 233:119784
Wang Y, Wu B, Zheng X, Chen B, Chu C (2023b) Assessing the quantum yield spectrum of photochemically produced reactive intermediates from black carbon of various sources and properties. Water Res 229:119450
Wang Z, Lin X, Yang K, Lin D (2024) Differential photodegradation processes of adsorbed polychlorinated biphenyls on biochar colloids with various pyrolysis temperatures. Water Res 251:121174
Wang X, Lin M, Peckmann J, Bayon G, Liang Q, Roberts HH, Feng D (2025) Black carbon formation at cold seeps and its potential contribution to the marine black carbon budget. Environ Sci Technol 59(16):7983–7992
Wei S, Zhu M, Fan X, Song J, Peng P, Li K, Jia W, Song H (2019) Influence of pyrolysis temperature and feedstock on carbon fractions of biochar produced from pyrolysis of rice straw, pine wood, pig manure and sewage sludge. Chemosphere 218:624–631
Wei J, Tu C, Yuan G, Zhou Y, Wang H, Lu J (2020a) Limited Cu(II) binding to biochar DOM: evidence from C K-edge NEXAFS and EEM-PARAFAC combined with two-dimensional correlation analysis. Sci Total Environ 701:134919
Wei P, Xu F, Fu H, Qu X (2020b) Impact of origin and structure on the aggregation behavior of natural organic matter. Chemosphere 248:125990
Wu H, Dong X, Liu H (2018) Evaluating fluorescent dissolved organic matter released from wetland-plant derived biochar: effects of extracting solutions. Chemosphere 212:638–644
Xia Y, Niu S, Yu J (2023) Microplastics as vectors of organic pollutants in aquatic environment: a review on mechanisms, numerical models, and influencing factors. Sci Total Environ 887:164008
Xia F, Liu Z, Zhang Y, Li Q, Zhao M, He H, Bao Q, Chen B, He Q, Lai C, He X, Ma Z, Zhou Y (2024) Calcium regulates the interactions between dissolved organic matter and planktonic bacteria in Erhai Lake, Yunnan Province, China. Water Res 261:121982
Xiang L, Harindintwali JD, Wang F, Redmile-Gordon M, Chang SX, Fu Y, He C, Muhoza B, Brahushi F, Bolan N, Jiang X, Ok YS, Rinklebe J, Schaeffer A, Zhu YG, Tiedje JM, Xing B (2022) Integrating biochar, bacteria, and plants for sustainable remediation of soils contaminated with organic pollutants. Environ Sci Technol 56(23):16546–16566
Xie W, Zhang S, Ruan L, Yang M, Shi W, Zhang H, Li W (2017) Evaluating soil dissolved organic matter extraction using three-dimensional excitation-emission matrix fluorescence spectroscopy. Pedosphere 27(5):968–973
Xin D, Li W, Choi J, Yu YH, Chiu PC (2023) Pyrogenic black carbon suppresses microbial methane production by serving as a terminal electron acceptor. Environ Sci Technol 57(49):20605–20614
Xing J, Qi Z, Dong W, Chen Q, Wu M, Yi P, Pan B, Xing B (2023) Aggregation of biochar nanoparticles and the impact on bisphenol A sorption: experiments and molecular dynamics simulations. Sci Total Environ 875:162724
Xu F, Wei C, Zeng Q, Li X, Alvarez PJJ, Li Q, Qu X, Zhu D (2017) Aggregation behavior of dissolved black carbon: implications for vertical mass flux and fractionation in aquatic systems. Environ Sci Technol 51(23):13723–13732
Xu F, Yao Y, Alvarez PJJ, Li Q, Fu H, Yin D, Zhu D, Qu X (2019) Specific ion effects on the aggregation behavior of aquatic natural organic matter. J Colloid Interf Sci 556:734–742
Xu Y, Ou Q, Liu C, Zhou X, He Q, Wu Z, Huang R, Ma J, Lu D, Huangfu X (2020) Aggregation and deposition behaviors of dissolved black carbon with coexisting heavy metals in aquatic solution. Environ Sci Nano 7(9):2773–2784
Xu Y, Ou Q, He Q, Wu Z, Ma J, Huangfu X (2021) Influence of dissolved black carbon on the aggregation and deposition of polystyrene nanoplastics: comparison with dissolved humic acid. Water Res 196:117054
Xu Y, Wang X, Ou Q, Zhou Z, van der Hoek JP, Liu G (2024) Appearance of recalcitrant dissolved black carbon and dissolved organic sulfur in river waters following wildfire events. Environ Sci Technol 58(16):7165–7175
Yamashita Y, Nakane M, Mori Y, Nishioka J, Ogawa H (2022) Fate of dissolved black carbon in the deep Pacific Ocean. Nat Commun 13(1):307
Yan C, Li Y, Sharma P, Chen Q, Li B, Shang J (2022) Influence of dissolved organic matter, kaolinite, and iron oxides on aggregation and transport of biochar colloids in aqueous and soil environments. Chemosphere 306:135555
Yan C, Wang W, Nie M, Ding M, Wang P, Zhang H, Huang G (2023) Characterization of copper binding to biochar-derived dissolved organic matter: effects of pyrolysis temperature and natural wetland plants. J Hazard Mater 442:130076
Yang F, Xu Z, Yu L, Gao B, Xu X, Zhao L, Cao X (2018) Kaolinite enhances the stability of the dissolvable and undissolvable fractions of biochar via different mechanisms. Environ Sci Technol 52(15):8321–8329
Yang W, Shang J, Sharma P, Li B, Liu K, Flury M (2019) Colloidal stability and aggregation kinetics of biochar colloids: effects of pyrolysis temperature, cation type, and humic acid concentrations. Sci Total Environ 658:1306–1315
Yang F, Zhang Q, Jian H, Wang C, Xing B, Sun H, Hao Y (2020a) Effect of biochar-derived dissolved organic matter on adsorption of sulfamethoxazole and chloramphenicol. J Hazard Mater 396:122598
Yang Z, Sun T, Subdiaga E, Obst M, Haderlein SB, Maisch M, Kretzschmar R, Angenent LT, Kappler A (2020b) Aggregation-dependent electron transfer via redox-active biochar particles stimulate microbial ferrihydrite reduction. Sci Total Environ 703:135515

Yang W, Li B, Shang J (2022) Aggregation kinetics of biochar nanoparticles in aqueous environment: interplays of anion type and bovine serum albumin. Sci Total Environ 833:155148
Yang S, Cao Y, Li Z, Ma C, Huang Y, Hu D, Liu H, Huangfu X (2024) Cotransport of aged biochar colloids and thallium(I) in water-saturated porous media: impact of the ionic strength, pH and aging degree. Sci Total Environ 927:172294
Yao J, Wang H, Fang J, Shan S, Joseph SD, van Zwieten L, Zhu K, Chen D, Jia H (2025) Distribution hotspots, formation mechanisms, and ecological effects of reactive oxygen species in soil and sediment: a critical review. Environ Sci Technol 59(27):13551–13565
Yin S, Wei C, Qu X, Fu H, Li B, Piao S, Tao S, Hatcher PG, Zhu D (2023) Benzenepoly(carboxylic acid)s as exclusive intrinsic markers to assess riverine export of dissolved black carbon. Environ Sci Technol 58(2):1142–1151
Yu Y, Li J (2024) Biochar-derived dissolved and particulate matter effects on the phytotoxicity of polyvinyl chloride nanoplastics. Sci Total Environ 906:167258
Yuan Q, Chen B, Hu Z, Wang L, Kong Q, Lian J, Wu H (2025) Effects of microplastics on atrazine removal in constructed wetlands: insight into the response characteristics of microorganisms, enzyme activity, and functional genes. Water Res 282:123730
Zhang P, Huang P, Xu X, Sun H, Jiang B, Liao Y (2020) Spectroscopic and molecular characterization of biochar-derived dissolved organic matter and the associations with soil microbial responses. Sci Total Environ 708:134619
Zhang R, Deng Z, Li J, Zhang Y, Wei Z, Cao H (2022) Effect of leaching time on phytotoxicity of dissolved organic matter derived from black carbon based on spectroscopy. Environ Pollut 307:119595
Zhang J, Zhou Z, Zeng L, Wang C, Han R, Ren X, Wang W, Xiang M, Chen S, Li H (2024a) The molecular binding sequence transformation of soil organic matter and biochar dissolved black carbon antagonizes the transport of 2,4,6-trichlorophenol. Sci Total Environ 947:174657
Zhang Z, Cui X, Qu X, Fu H, Tao S, Zhu D (2024b) Revealing molecular structures of nitrogen-containing compounds in dissolved black carbon using ultrahigh-resolution mass spectrometry combined with thermodynamic calculations. Environ Sci Technol 58(27):11998–12007
Zhao K, Shang J (2023) Transport of biochar colloids under unsaturated flow condition: roles of chemical aging and cation type. Sci Total Environ 859(2):160415
Zhao K, Gao L, Zhang Q, Shang J (2021) Accumulation of sulfamethazine and ciprofloxacin on grain surface decreases the transport of biochar colloids in saturated porous media. J Hazard Mater 417:125908
Zhou P, Tian L, Graham N, Song S, Zhao R, Siddique MS, Hu Y, Cao X, Lu Y, Elimelech M, Yu W (2024) Spatial patterns and environmental functions of dissolved organic matter in grassland soils of China. Nat Commun 15(1):6356
Zhou H, Wang H, Wang H, Wang X, Ye Z, Hu X (2025) Indirect photodegradation of pharmaceutical and personal care products in dissolved black carbon solution: the role of microheterogeneous distribution of hydroxyl radical and sorption. Water Res 268(B):122685